EARTHQUAKE ENGINEERING AND STRUCTURAL DYNAMICS
Earthquake Engng Struct. Dyn. 2009; **38**:1009–1026
Published online 12 December 2008 in Wiley InterScience (www.interscience.wiley.com). DOI: 10.1002/eqe.880

A study on using pre-bent steel strips as seismic energy-dissipative devices

Yen-Po Wang*,† and Chia-Shang Chang Chien

Department of Civil Engineering, National Chiao-Tung University, Hsinchu, Taiwan

SUMMARY

Buckling is usually conceived as an unstable structural behavior leading to lateral instability of axially loaded members, if not properly supported. However, a pre-bent strip would become an excellent seismic energy-dissipative device if it is deformed in a guided direction and range. Geometrically large lateral deformation of the steel strips in buckling leads to inelastic behavior of the material and dissipates energy as a consequence. The purpose of this study is to propose a new type of seismic damper in the form of braces based on pre-bent steel strips. The nonlinear elastic stiffness of monotonously loaded pre-bent strips in both compression and tension is derived. The energy-dissipative characteristics of the proposed damping device are investigated via component tests under cyclic loads. Experimental results indicate that the force–displacement relationship of pre-bent strips in cyclic loads exhibits mechanical characteristics of displacement-dependent dampers. A series of seismic performance tests has been conducted further to verify the feasibility and effectiveness of using the proposed device as seismic dampers. Encouraging test results have been obtained, suggesting feasibility of the proposed device for earthquake-resistant design.

Received 3 June 2008; Revised 26 October 2008; Accepted 29 October 2008

KEY WORDS: buckling; pre-bent strip; buckling-type energy-dissipative damper; hysteretic loops; shaking table test

INTRODUCTION

Mitigation of machine-induced vibration via isolation with pre-bent struts has been studied in recent years [1–5]. Pre-bent struts are made of metallic strips bent into an arch shape whose stiffness decreases with increasing curvature of the arch. A pre-bent strut-controlled system under the motion of foundation is illustrated in Figure 1, in which the pre-bent strut is working as a geometrically

*Correspondence to: Yen-Po Wang, Department of Civil Engineering, National Chiao-Tung University, Hsinchu, Taiwan.
†E-mail: ypwang@mail.nctu.edu.tw

Contract/grant sponsor: National Science Council, Republic of China; contract/grant numbers: NSC96-2625-Z-009-003, NSC96-2622-E-009-007-CC3

nonlinear spring by changing its stiffness with the reciprocating motion for frequency adjustment of the system. Virgin and Davis [2] developed a vibration isolation system using two parallel simply-supported buckled struts. In terms of the power spectral density of vertical responses, the experimental results of the buckled struts under harmonic excitations at various frequencies proved effective in reducing high-frequency excitations. Chin *et al*. [3] also adopted the pre-bent struts as vertical springs, as shown in Figure 2, to reduce the vibration of a vertical stage. Gao *et al*. [5] studied the energy-absorbing behavior of pre-bent plates under impact loading. A simplified one-dimensional mass-spring model with variable mass was proposed based on a rigid, perfectly plastic model. The predicted displacement responses of the striker by the simplified mass-spring model agreed very well with those obtained by the FE model using ABAQUS. Plaut *et al*. [6] considered a pre-bent column with clamped ends as the vibration isolator. The effects of weight and initial curvature of the pre-bent columns on the displacement transmissibility were explored. Plaut *et al*. [7] and Jeffers *et al*. [8] further investigated the control effectiveness of either a single-column isolator or double-column isolator bonded with viscoelastic filler on a horizontal rigid bar under simple-harmonic base motion in the vertical direction. It was concluded that the isolators could be

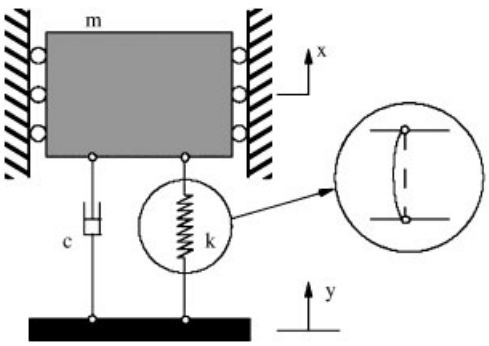

Figure 1. Schematic diagram of a mass isolated with buckled struts [2].

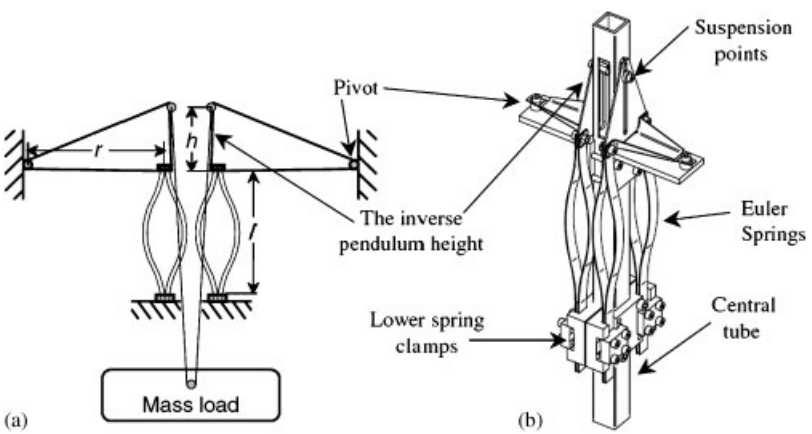

Figure 2. Vertical isolation stage with Euler spring [3].

DOI: 10.1002/eqe

effective for a large range of excitation frequencies. The pre-bent column isolators were further extended for the isolation of a horizontal rigid plate in 3-D motions under both free vibration and harmonic excitation. Ibrahim *et al*. [9] proposed a similar visco-plastic damper consisting of a block of high-damping rubber sandwiched between two pre-bent steel plates for seismic protection of structures. Ji and Hansen [10] investigated the mechanical characteristics of the pre-bent struts with one end fixed and the other free to slide. The friction at the sliding end was adjusted to regulate the damping of the system. Bonello *et al*. [11] proposed an adaptive tuned vibration absorber (ATVA) consisting of piezo-actuator and buckled struts. The stiffness of the ATVA could be actively adjusted to change the vibration frequency of the system.

Despite buckling being commonly conceived as an unstable structural behavior leading to lateral instability of axially loaded members, a pre-bent strip would become an excellent seismic energy-dissipative device if deformed in a guided direction and range. The pre-bent strips investigated so far, however, were considered mostly as spring elements for vibration isolation of equipment. When axially loaded, the pre-bent strips are subjected to geometrically large lateral deformation that may in turn cause the material to deform inelastically, and become energy-dissipative under cyclic loads. This makes it a potential candidate for a seismic structural damper.

The purpose of this study is to develop the fundamental principles of a pre-bent strip and investigate its potential as a seismic damper. The nonlinear elastic stiffness of monotonously loaded pre-bent strips in both compression and tension is derived. The energy-dissipative characteristics of the pre-bent steel strips are investigated via component tests. A seismic damper based on the pre-bent strips is further developed, and a series of seismic performance tests with a shaking table is conducted to verify the feasibility of using pre-bent strips in the form of braces for seismic structural control. In contrast to the buckling-restrained brace (BRB) [12, 13] meant to prevent the braces from buckling, the proposed device allows for in-plane buckling localized in the segment of pre-bent strips. The BRBs are structural members that contribute substantial lateral stiffness to moment-resisting frames. They may dissipate seismic energy, if axially loaded to yield in strong earthquakes. The braces with pre-bent strips, on the other hand, are not designed for stiffness reinforcement of the structural system, but only as a supplemental damping device in which the pre-bent strips are to yield at relatively small axial forces. In this way, the proposed device can effectively dissipate seismic energy in earthquakes at early stages.

NONLINEAR ELASTIC BUCKLING STIFFNESS OF PRE-BENT STRIPS

The pre-bent strip considered in this study is a single steel strip with initial camber as illustrated in Figure 3. Provided that both the ends of the pre-bent strip are clamped, the deformed shape of the pre-bent strip in Figure 4 can be approximated in terms of the chord–tangent angle function, $\theta(s)$, as

$$\theta(s) = qF(s) \tag{1}$$

where

$$F(s) = \sin\left(\frac{2\pi s}{L}\right) - \frac{L}{2} \leqslant s \leqslant \frac{L}{2} \tag{2}$$

in which L is the arc length of the pre-bent strip and q is the slope of the tangent at the inflection point at $s = L/4$.

DOI: 10.1002/eqe

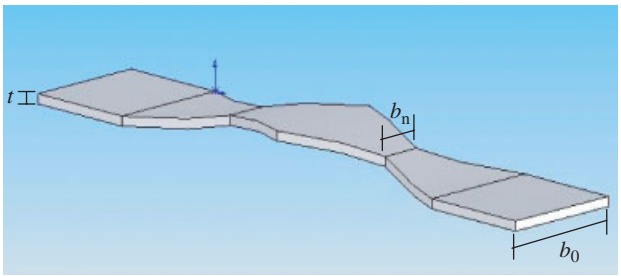

Figure 3. Configuration of a single pre-bent metallic strip.

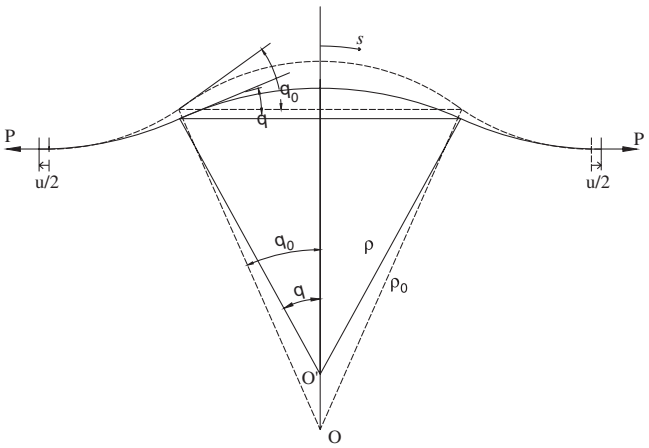

Figure 4. Pre-bent strip before and after loaded in tension.

The initial chord–tangent angle, $\theta_0(s)$, before the external axial force is applied can be represented by using Equation (1) as

$$\theta_0(s) = q_0 F(s) \tag{3}$$

where q_0 is the initial slope of the strip at the inflection point.

The axial deformation of the pre-bent strip subjected to an axial force, P, can be calculated as

$$u(q) = \int_{-L/2}^{+L/2} [\cos(\theta(s)) - \cos(\theta_0(s))]\,\mathrm{d}s$$

$$= \int_{-L/2}^{+L/2} \left[\cos\left(q \sin\left(\frac{2\pi s}{L}\right)\right) - \cos\left(q_0 \sin\left(\frac{2\pi s}{L}\right)\right)\right] \mathrm{d}s \tag{4}$$

DOI: 10.1002/eqe

Carrying out the integration of Equation (4) by using the Taylor series expansion without the high-order terms, the slope q can be written in terms of q_0 and u as

$$q = \left[q_0^2 - \frac{2u}{L} \right]^{1/2} \tag{5}$$

Moreover, the strain energy, U^{S}, and the elastic potential energy, U^{P}, can be further obtained, respectively as

$$U^{\mathrm{S}}(q) = \frac{1}{2} E \int_{-L/2}^{+L/2} I(s)(\theta' - \theta_0')^2 \, \mathrm{d}s = \frac{1}{2} E \int_{-L/2}^{+L/2} I(s)(q - q_0)^2 (F')^2 \, \mathrm{d}s \tag{6}$$

$$U^{\mathrm{P}}(q) = -Pu(q) = P \int_{-L/2}^{+L/2} [\cos(q_0 F) - \cos(qF)] \, \mathrm{d}s \tag{7}$$

where E is Young's modulus of the material, and

$$I(s) = \tfrac{1}{12} b(s) t^3 \tag{8}$$

is the area moment of inertia at any arbitrary position, s, of the pre-bent strip, t is the thickness of the strip and $b(s)$ is the width at the corresponding position. If the width of the strip is varied linearly in four equal segments with necking toward the two inflection points, then

$$b(s) = \begin{cases} \dfrac{-4b_0}{L}(1-\beta)s + b_0(2\beta - 1) & \text{for } -\dfrac{L}{2} \leqslant s \leqslant -\dfrac{L}{4} \\ \dfrac{4b_0}{L}(1-\beta)s + b_0 & \text{for } -\dfrac{L}{4} \leqslant s \leqslant 0 \\ \dfrac{-4b_0}{L}(1-\beta)s + b_0 & \text{for } 0 \leqslant s \leqslant +\dfrac{L}{4} \\ \dfrac{4b_0}{L}(1-\beta)s + b_0(2\beta - 1) & \text{for } +\dfrac{L}{4} \leqslant s \leqslant +\dfrac{L}{2} \end{cases} \tag{9}$$

in which $\beta = b_{\mathrm{n}}/b_0$ is the ratio of the original strip width, b_0, to the neck width, b_{n}, indicated in Figure 3.

Taking both the strain and elastic potential energy into account, the total potential energy can be represented as

$$V(q) = U^{\mathrm{S}}(q) + U^{\mathrm{P}}(q) \tag{10}$$

The axial force P can be found by using the theory of least work [14] as the following:

$$\frac{\partial V(q)}{\partial q} = E \int_{-L/2}^{+L/2} I(s)(q - q_0) F'^2 \, \mathrm{d}s + P \int_{-L/2}^{+L/2} F \sin(qF) \, \mathrm{d}s = 0 \tag{11}$$

Consequently, the axial force P is obtained from Equation (11) as

$$P = -\frac{E \int_{-L/2}^{+L/2} I(s)(q - q_0)(F')^2 \, \mathrm{d}s}{\int_{-L/2}^{+L/2} [F \sin(qF)] \, \mathrm{d}s} \tag{12}$$

DOI: 10.1002/eqe

Carrying out the integration of Equation (12) by using the Taylor series expansion without the high-order terms leads to

$$P = P_{\mathrm{cr}}\left(1-\frac{q_0}{q}\right)\left(\frac{1}{4}(1+\beta)+\frac{1}{\pi^2}(1-\beta)\right)\left(-1+\frac{q^2}{8}\right)^{-1} \tag{13}$$

in which $P_{\mathrm{cr}}=4\pi^2 EI/L^2$, where $I=bt^3/12$.

Substituting Equation (5) for q into Equation (13), the axial force, P, can be further represented as

$$P = P_{\mathrm{cr}}\left[1-q_0\left(q_0^2-\frac{2u}{L}\right)^{-1/2}\right]\left(\frac{1}{4}(1+\beta)+\frac{1}{\pi^2}(1-\beta)\right)\left(-1-\frac{u}{4L}+\frac{1}{8}q_0^2\right)^{-1} \tag{14}$$

Finally, the equivalent nonlinear elastic stiffness of the pre-bent strip can be implicitly represented as

$$K(q_0, u, \beta) = \frac{P(q_0, u, \beta)}{u} \tag{15}$$

A parametric study is conducted further to explore the effects of initial slope, arc length and shaping in terms of the width ratio ($\beta = b_{\mathrm{n}}/b_0$) on the mechanical characteristics of the pre-bent strips. Figure 5 shows the force–displacement relationship of the pre-bent strips with different initial slope ($q_0 = 0.41$, 0.33 and 0.27 rad) of the chord-tangent at the inflection point. The axial displacement is positive in tension and negative in compression. It is observed that the stiffness of the pre-bent strip tends to increase with larger axial displacement when loaded in tension from the initial configuration, while it decreases with larger displacement when loaded in compression. The result also indicates that the stiffness of the pre-bent strip with a smaller initial slope tends to increase at a faster rate in tension, while it decreases at a slower rate in compression. It is noted that for the case with $q_0 = 0.27$ rad, the maximum axial displacement in tension is only 23.69 mm, beyond which Equation (14) is no longer valid because the arch will be completely flattened. Figure 6 shows the force–displacement relationship of the pre-bent strips with different arc length ($L = 600$, 650 and 700 mm). The result indicates that the stiffness of the pre-bent strip with a

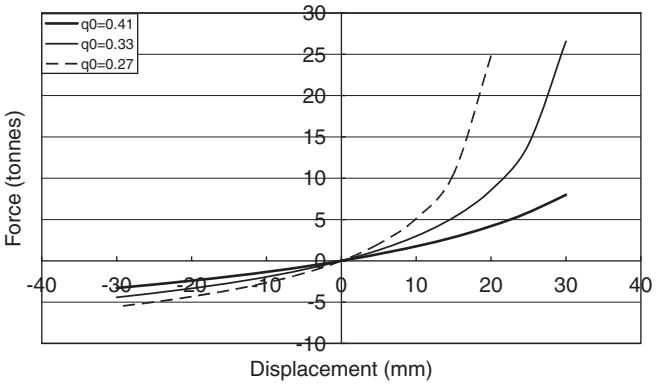

Figure 5. Force–displacement relationship of the pre-bent strips for various initial slope ($L = 650$ mm, $t = 12$ mm, $b = 150$ mm, $\beta = 0.33$, $E = 2.0 \times 10^5$ MPa).

DOI: 10.1002/eqe

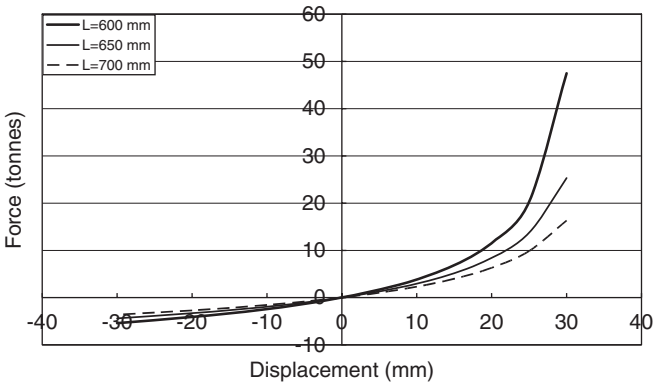

Figure 6. Force–displacement relationship of the pre-bent strips at various length ($t=12\,\text{mm}$, $b=150\,\text{mm}$, $\beta=0.33$, $q_0=0.33$, $E=2.0\times10^5\,\text{MPa}$).

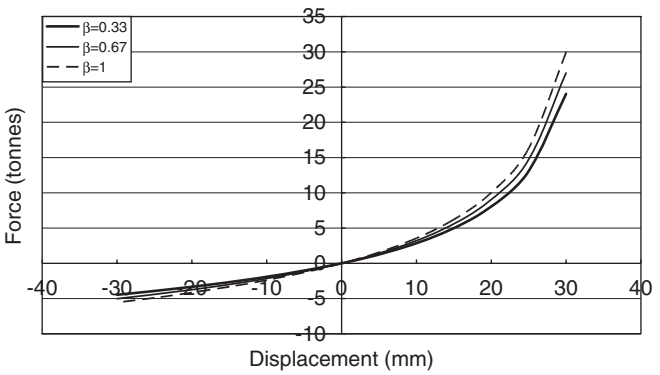

Figure 7. Force–displacement relationship of the pre-bent strips at various β ($L=650\,\text{mm}$, $t=12\,\text{mm}$, $b=150\,\text{mm}$, $q_0=0.33$, $E=2.0\times10^5\,\text{MPa}$).

smaller arc length tends to increase at a faster rate in tension, while it decreases at a slower rate in compression. Moreover, the force–displacement relationship of the pre-bent strip for different β ($\beta=0.33$, 0.67 and 1) in Figure 7 indicates that the stiffness of the pre-bent strip tends to increase with larger β. The features of the pre-bent strip explored from the above parametric study are useful for design considerations.

COMPONENT TESTS

To further investigate the energy-dissipative characteristics of the proposed damping device in full scale, a series of component tests on the pre-bent strips has been conducted. First, a single unit of pre-bent strip is tested in a non-symmetric layout. It is followed by the testing of a coupled unit

DOI: 10.1002/eqe

of the pre-bent strips in a symmetric layout in a sense that the integrated mechanical behavior of the coupled unit becomes symmetric with respect to the neutral position.

Single unit of pre-bent strip in a non-symmetric layout

The design detail of the pre-bent strip used in the component test is illustrated in Figure 8. A single unit of pre-bent strip pair in parallel is tested in a non-symmetric layout as in nature the mechanical behavior of the pre-bent strip in tension differs from that in compression. The experimental setup for the component test is shown in Figure 9. The seating H-beam of the testing frame is fixed to the strong floor while the movable upper part is connected to a hydraulic actuator, which in turn is clamped on the other end against the SRC reacting wall. The pre-bent strip pair is connected to the seating H-beam in one end and to the movable upper part in the other via brackets. The cyclic loading test is conducted in a displacement-controlled mode with the amplitudes set sequentially to be 5, 10, 15, 20, 25 and 30 mm at a loading rate of 0.2 mm/s. Three repetitions of triangular waves at each of the designated amplitudes are completed continuously before proceeding to the next stage.

The hysteresis (restoring force vs axial displacement) of the pre-bent strips obtained under cyclic loading shown in Figure 10(a) reveals desirable energy-dissipative characteristics of the pre-bent strips. Consistency of the repeated trajectories at each of the designated amplitudes indicates a stable mechanical behavior of the pre-bent strips under cyclic loading conditions. The stiffness increases with displacement in tension and decreases in compression, as in a monotonous static loading condition previously disclosed in the parametric study.

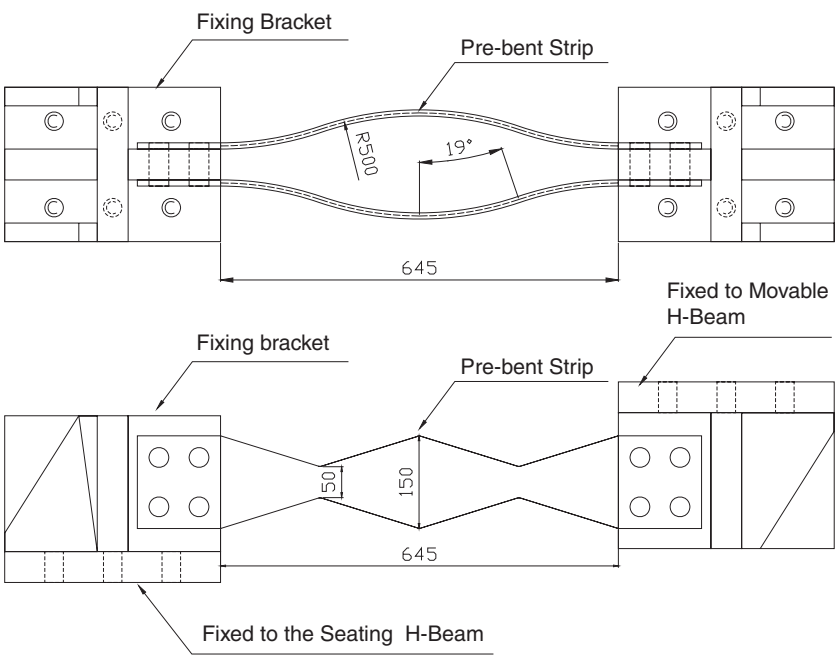

Figure 8. Details of the pre-bent strip pair tested in a non-symmetric layout (unit: mm).

DOI: 10.1002/eqe

Figure 9. Experimental setup for component test of a pre-bent strip pair in a non-symmetric layout.

Numerical prediction of the test result is further conducted using ANSYS with a bilinear stress–strain model of mild steel in which Young's Modulus of 2×10^5 MPa, the yielding stress and strain respectively of 2.35×10^2 MPa and 0.001175, and a post-yielding stiffness ratio of 0.01 are considered. The SOLID186 element is adopted in the modeling of the pre-bent strip. In order to simulate the boundary condition of an axially loaded pre-bent strip in a displacement-controlled loading test, the nodal displacements at one end of the strip are fixed in all three directions (x, y, z) and allowed to slide only in the axial direction (x) at the other end. The cyclic loading process is represented by imposing sliding displacement at the movable end of the strip in the form of triangular waves corresponding to the component test. The axial forces developed in reaction to the imposed displacements are presented in hysteresis loops as illustrated in Figure 10(b) and compared with those obtained from the test. Large discrepancy between the test and simulated results has been observed, in particular the portion of the unloading paths where the analytical

DOI: 10.1002/eqe

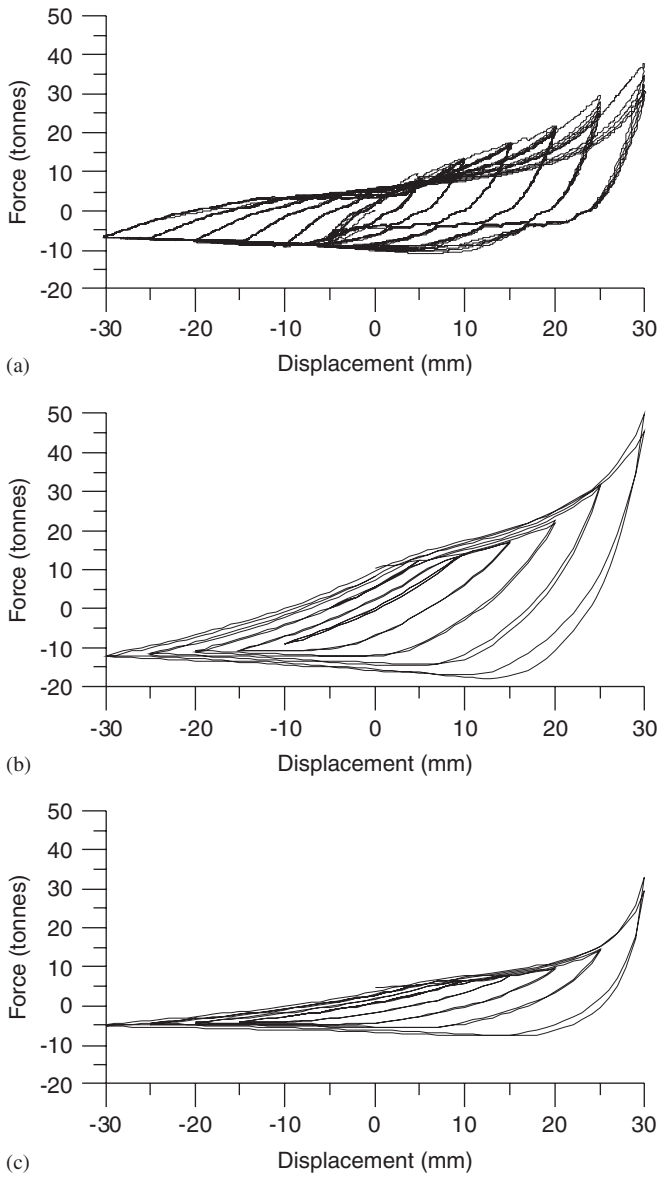

Figure 10. Hysteresis of the pre-bent strip under cyclic loads in a non-symmetric layout: (a) experimental; (b) ANSYS-clamped; and (c) ANSYS-hinged.

prediction exhibits more pronounced energy-dissipative capability. Possible explanations for the discrepancy are

(a) The boundary condition of the strip is not perfectly 'clamped' as ideally assumed in the simulation. The actual boundary condition of the tested pre-bent strip is between a 'hinged'

DOI: 10.1002/eqe

and 'clamped' condition. This may reduce the yielded portion of the material as otherwise in a fully clamped condition, and thus provide less energy-dissipative capacity.

(b) Inevitable rotation of the movable H-beam and slippage at the bolted connections during the test did occur, although it was considered moderate.

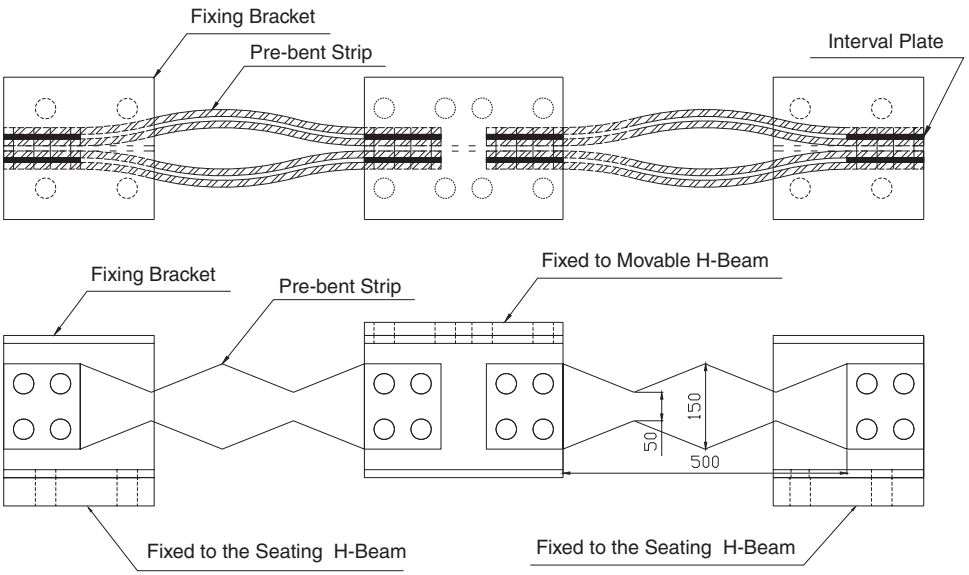

Figure 11. Details of the coupled pre-bent strip units tested in a symmetric layout (unit: mm).

Figure 12. Experimental setup for component test of coupled pre-bent strips in a symmetric layout.

DOI: 10.1002/eqe

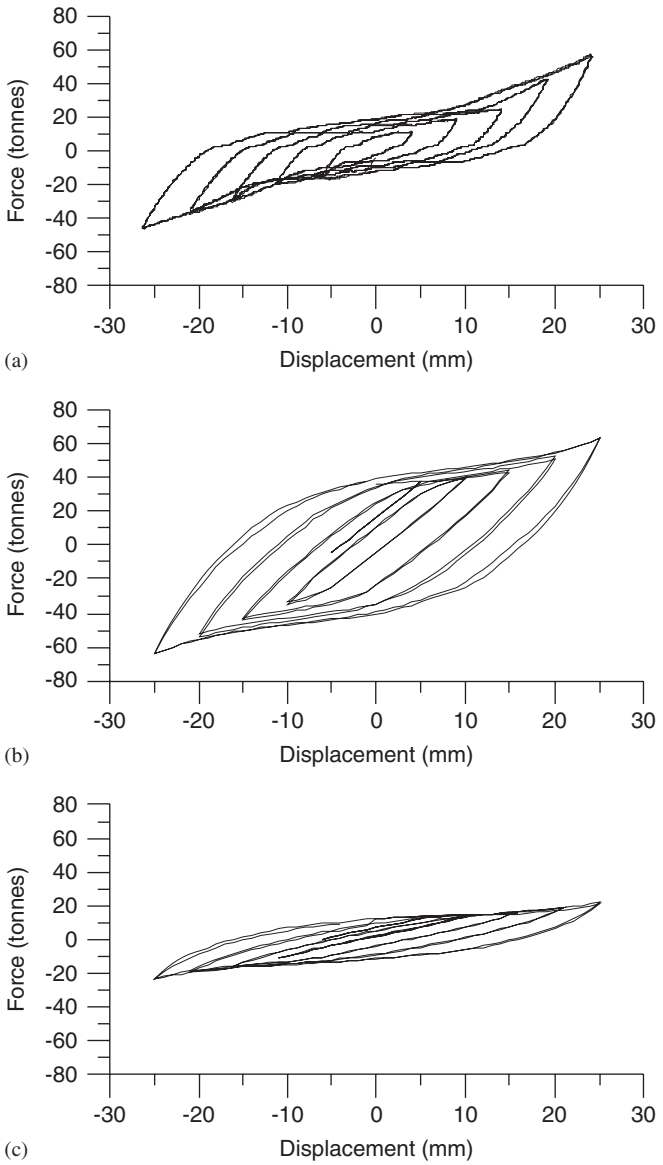

Figure 13. Hysteresis of the coupled units of pre-bent strips under cyclic loads: (a) experimental; (b) ANSYS-clamped; and (c) ANSYS-hinged.

To gain more insight into the effect of boundary conditions on the inelastic behavior of the pre-bent strip, analytical simulation of the pre-bent strip with a hinged condition is carried out. The enclosed area of the hysteresis in Figure 10(c) for the hinged strip is flatter in comparison with that for the clamped one, indicating less energy dissipation. Moreover, the test result is between those of the clamped and hinged conditions. This is reasonable since the actual boundary condition

DOI: 10.1002/eqe

Figure 14. Experimental setup of a 5-story model frame implemented with pre-bent strips.

of the pre-bent strip is not perfectly clamped as intended in the design. The energy-dissipative capacity of the pre-bent strip may be improved, if the end connection could be welded in addition to bolting to make it closer to a clamped condition.

Coupled unit of pre-bent strip in a symmetric layout

The structural behavior of pre-bent steel strips is in nature non-symmetric, as also revealed from the above test results. It is important, however, to maintain a symmetric structural behavior of the seismic damping devices for design purpose. This can be achieved by properly arranging the implementation layout of the dampers in symmetric pairs. The component test of coupled units of pre-bent steel strip in a symmetric layout is conducted further. The design detail of the coupled pre-bent strip units with multiple pieces on each side is illustrated in Figure 11, and the corresponding experimental setup is shown in Figure 12. In this manner, the two units will be subjected to axial forces in opposite directions during the loading process. The same cyclic loading history as in the previous test is considered. The reaction force then measured from the built-in load cell of the actuator is the sum of axial forces in the coupled units.

The hysteresis (restoring force vs axial displacement) of the coupled pre-bent strip units obtained under cyclic loading shown in Figure 13(a) reveals desirable energy-dissipative characteristics. Consistency of the repeated trajectories at each of the designated amplitudes again indicates a stable mechanical behavior of the pre-bent steel strips. As expected, the integrated restoring forces of the coupled units as a whole are symmetric with respect to the neutral position.

Numerical prediction of the test result is also conducted using ANSYS with the same bilinear stress–strain model considered earlier. The coupled strip units are aligned in series with one end

DOI: 10.1002/eqe

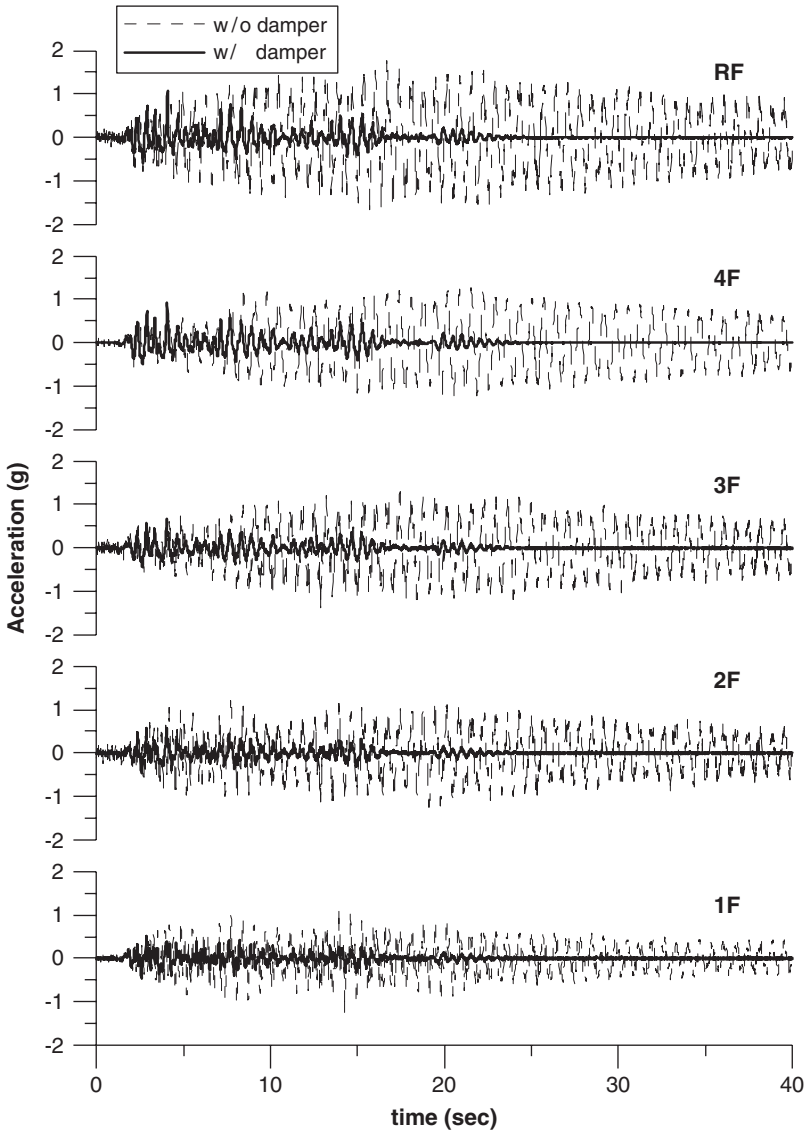

Figure 15. Comparison of the seismic acceleration responses with and without the proposed damping device (input: El Centro, PGA $= 0.5g$).

overlapped with each other in the middle of the layout. The sliding displacement is imposed on the middle (overlapped) point with the other ends fixed to simulate the test condition that the axial forces in each of the coupled units are always opposite in direction.

The axial forces developed in reaction to the imposed displacements are presented in hysteresis loops and compared with those obtained from the test, as illustrated in Figure 13(b). The analytical prediction again exhibits more pronounced energy-dissipative capability than the test result.

DOI: 10.1002/eqe

Analytical simulation of the coupled pre-bent strip units with a hinged condition is further carried out. The enclosed area of the hysteresis in Figure 13(c) for the hinged strip is flatter in comparison with that for the clamped one, and the energy-dissipative capability of the test result is between those of the clamped and hinged conditions.

SEISMIC PERFORMANCE TEST

As a further step in exploring the feasibility of applying pre-bent steel strips for seismic vibration control, a series of seismic performance tests is conducted using a uni-axial shaking table of 10-ton payload. A 5-story model frame implemented with pre-bent strips (Figure 14) in the form of braces is tested under two of the benchmark earthquakes, namely the 1940 El Centro and 1995 Kobe, specified by the International Structural Control Society. Accelerometers were implemented on each floor to monitor the acceleration responses. A dynamic load cell of Jihsense (model number: LM-2T) with a capacity of 2000 kg is installed in series with each ductile brace in the first story to measure the resulting axial force. Moreover, a laser displacement sensor of Wenglor with a dynamic range of ± 15 cm is installed on each diagonal brace in the first story to monitor its axial displacement. The model structure without the damping device is tested with a moderate earthquake intensity at PGA $= 0.1g$ to avoid damage. The recorded seismic responses are scaled to the level of intensity under which the model structure facilitated with the damping device is tested for comparison.

Figure 15 shows the seismic floor accelerations of the 5-story building frame under El Centro earthquake with PGA $= 0.5g$. Significant reduction of the acceleration responses has been observed at all floors with the proposed damping devices implemented. As summarized in Table I, significant reduction of the peak floor acceleration ranging from 29 to 60% has been achieved, and the RMS acceleration has been reduced by over 70% throughout the floors. Figure 16 shows the seismic floor accelerations of the 5-story building frame under Kobe earthquake with PGA $= 0.4g$. Significant reduction of the acceleration responses has been observed at all floors with the braces implemented.

Table I. Comparison of floor acceleration in seismic performance test (input: El Centro earthquake, PGA $= 0.5g$).

Floor	w/o damper (g)	w/damper (g)	Reduction (%)
Peak response of acceleration			
1F	1.25	0.50	60
2F	1.23	0.59	52
3F	1.36	0.68	50
4F	1.28	0.91	29
5F	1.75	1.08	38
RMS response of acceleration			
1F	0.33	0.09	74
2F	0.47	0.09	81
3F	0.53	0.10	81
4F	0.58	0.13	77
5F	0.69	0.14	80

DOI: 10.1002/eqe

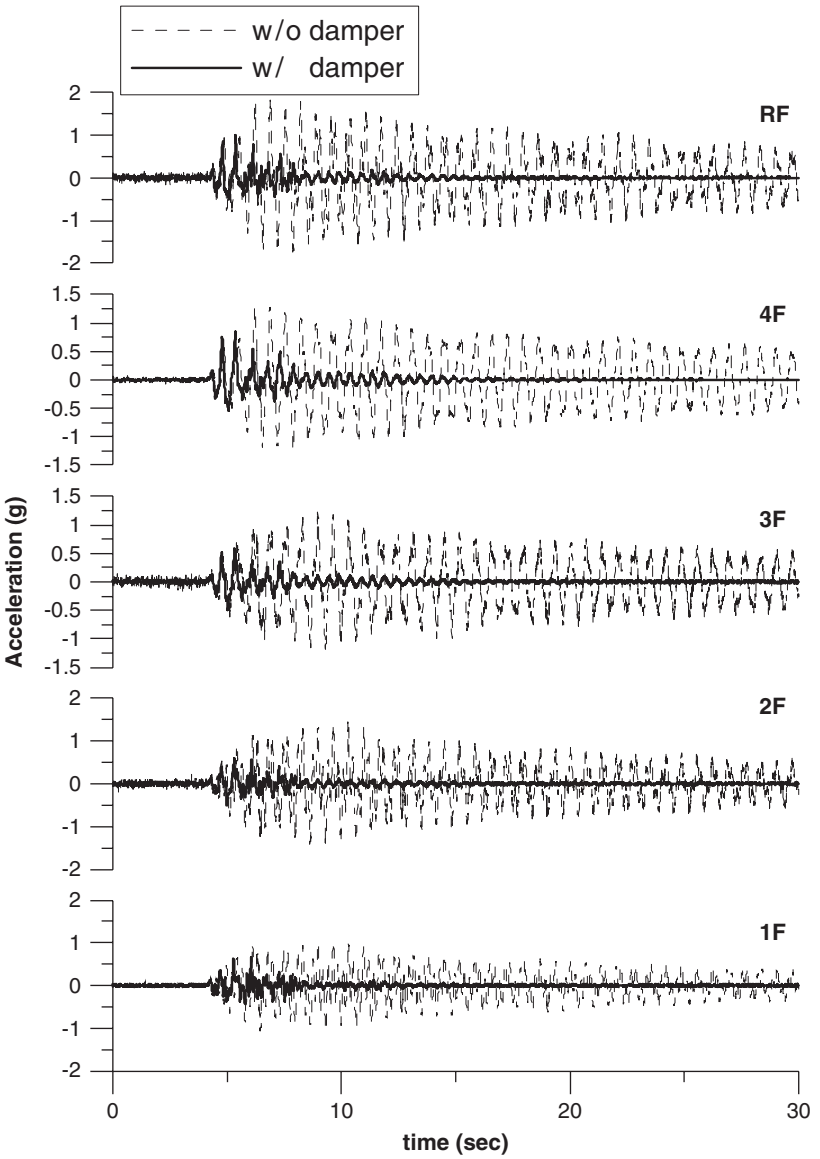

Figure 16. Comparison of the seismic acceleration responses with and without the proposed damping device (input: Kobe earthquake, PGA = 0.4g).

As summarized in Table II, significant reduction of the peak floor acceleration ranging from 34 to 59% has been achieved, and the RMS acceleration has been reduced by over 80% throughout the floors. The hysteresis from directly measured axial forces and displacements of the pre-bent strips in Figure 17 show a similar pattern as in the cyclic loading test. This is expected since the inelastic material behavior of the proposed damping device is rate-independent. The test results

DOI: 10.1002/eqe

Table II. Comparison of floor acceleration in seismic performance test (input: Kobe earthquake, PGA = 0.4g).

Floor	w/o damper (g)	w/damper (g)	Reduction (%)
Peak response of acceleration			
1F	1.07	0.67	37
2F	1.44	0.59	59
3F	1.23	0.59	52
4F	1.28	0.84	34
5F	1.82	1.01	45
RMS response of acceleration			
1F	0.30	0.06	80
2F	0.40	0.06	85
3F	0.39	0.06	84
4F	0.44	0.08	81
5F	0.54	0.09	84

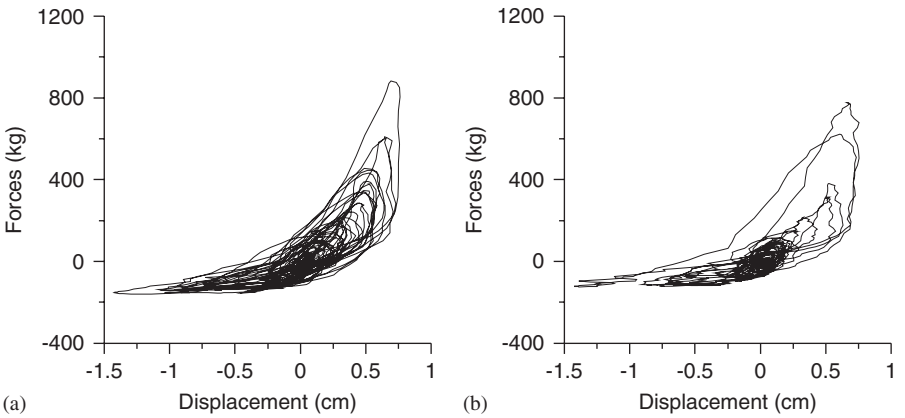

Figure 17. Hysteresis of the ductile brace with pre-bent strip in seismic performance tests: (a) El Centro earthquake, PGA = 0.5g and (b) Kobe earthquake, PGA = 0.4g.

confirm the effectiveness and feasibility of using pre-bent strips as energy-dissipative devices for seismic structural control in its present form.

CONCLUDING REMARKS

In this study, a new type of seismic structural damper in the form of braces based on pre-bent strips has been proposed. The nonlinear elastic stiffness of monotonously loaded pre-bent strips with both ends clamped is derived. The mechanical behavior of the pre-bent strips in nature is not symmetric with respect to the neutral position. Component tests in cyclic loading show that the force–displacement relationship (hysteresis loop) of the pre-bent strips is similar to those of the displacement-dependent metallic dampers. Symmetric structural behavior of the pre-bent

DOI: 10.1002/eqe

strips can be obtained, if properly arranged in couples. Although a discrepancy exists between the FEM simulation and test data, the seismic performance test results confirm the feasibility and effectiveness of using pre-bent steel strips as energy-dissipative devices for seismic structural control. In practical application, the energy-dissipative capacity of the pre-bent strips might be improved if the end connection could be welded in addition to bolting to make it closer to a clamped condition.

ACKNOWLEDGEMENTS

This work is partially supported by the National Science Council, Republic of China under contract NSC96-2625-Z-009-003 and NSC96-2622-E-009-007-CC3.

REFERENCES

1. Winterflood J, Blair D, Slagmolen B. High performance vibration isolation using springs in Euler column buckling mode. *Physics Letters A* 2002; **300**:122–130.
2. Virgin LN, Davis RB. Vibration isolation using buckled struts. *Journal of Sound and Vibration* 2003; **260**:965–973.
3. Chin EJ, Lee KT, Winterflood J, Jacob J, Blair DG, Ju L. Techniques for reducing the resonant frequency of Euler spring vibration isolations. *Classical and Quantum Gravity* 2004; **21**:959–963.
4. Winterflood J, Barber TA, Blair DG. Using Euler buckling spring for vibration isolation. *Classical and Quantum Gravity* 2002; **19**:1639–1645.
5. Gao ZY, Yu TX, Lu G. A study on type II structures. Part I: a modified one-dimensional mass-spring model. *International Journal of Impact Engineering* 2005; **31**:895–910.
6. Plaut RH, Sidbury JE, Virgin LN. Analysis of buckled and pre-bent fixed-end columns used as vibration isolators. *Journal of Sound and Vibration* 2005; **283**(3–5):1216–1228.
7. Plaut RH, Favor HM, Jeffers AE, Virgin LN. Vibration isolation using buckled or pre-bent columns. Part 1: two-dimensional motions of horizontal rigid bar. *Journal of Sound and Vibration* 2008; **310**:409–420.
8. Jeffers AE, Plaut RH, Virgin LN. Vibration isolation using buckled or pre-bent columns. Part 2: three-dimensional motions of horizontal rigid plate. *Journal of Sound and Vibration* 2008; **310**:421–432.
9. Ibrahim YE, Marshall J, Charney FA. A visco-plastic device for seismic protection of structures. *Journal of Constructional Steel Research* 2007; **63**:1515–1528.
10. Ji JC, Hansen CH. Non-linear response of a post-buckled beam subjected to a harmonic axial excitation. *Journal of Sound and Vibration* 2000; **237**(2):303–318.
11. Bonello P, Brennan MJ, Elliott SJ. Vibration control using an adaptive tuned vibration absorber with a variable curvature stiffness element. *Smart Materials and Structures* 2005; **14**(5):1055–1065.
12. Sabelli R, Mahin S, Chang C. Seismic demands on steel braced frame buildings with buckling-restrained braces. *Engineering Structures* 2003; **25**:655–666.
13. Qiang X. State of the art of buckling-restrained braces in Asia. *Journal of Constructional Steel Research* 2005; **61**:727–748.
14. Hsieh YY. *Elementary Theory of Structures* (3rd edn). Prentice-Hall: Englewood Cliffs, NJ, 1998.

DOI: 10.1002/eqe